Letter

Complex dispersion relation of Rayleigh-Bloch waves trapped by slow inclusions

Vincent Laude
Université Marie et Louis Pasteur, CNRS, Institut FEMTO-ST, F-25000 Besançon, France

(Received 4 March 2025; revised 12 May 2025; accepted 10 June 2025; published 20 June 2025)

Rayleigh-Bloch waves are guided acoustic waves propagating along a periodic line of inclusions placed inside an open, infinite medium. Below the sound cone, they are transversely evanescent on both sides of the line of inclusions. Guidance is then achieved without any cladding surrounding the segmented core. Inclusions usually impose definite boundary conditions, resulting in a single guided band. We consider instead the case of permeable, slow inclusions inside a fast medium. Introducing the concept of guided quasinormal modes, we obtain the complex dispersion relation taking into account radiation at infinity. We thus show that multiple bands of leaky Rayleigh-Bloch waves appear and that guided bound states in the continuum arise as a result of the combination of symmetry and periodicity.

DOI: 10.1103/195c-gy6f

Introduction. Rayleigh-Bloch (RB) waves are waves guided along a periodic chain of scatterers or inclusions inside an open, infinite, host medium [Fig. 1(a)] [1]. The significance of such an arrangement is that the chain acts as a guide and confines waves in space even though there is no physical boundary to contain them. In essence, the dispersion of Rayleigh-Bloch waves is not determined by boundary conditions but by the periodic distribution of inclusions. Denoting x the periodic axis (Fig. 1), guided modes of propagation are Bloch waves of the form $p(x,y)\exp[\imath(\omega t - kx)]$, with k the Bloch wave number and $p(x,y)$ a wave field periodic along axis x that decays exponentially in the positive and negative y direction. Strictly speaking, the dispersion of Rayleigh-Bloch waves lies only under the sound cone, the region of dispersion space for which waves have a phase velocity smaller than that of any bulk wave in the host medium. Rayleigh-Bloch waves have been discussed for many different physical systems, including surface water waves [2–5], thin elastic plates [6], and a one-dimensional infinite array of point masses on an infinite, thin elastic plate [7], whispering gallery modes [8], lines of acoustic resonators inside a thick plate [9], and acoustic diffraction gratings in air [10].

There have been several discussions of the relation of Rayleigh-Bloch waves to the trapped modes that appear due to rigid obstacles placed symmetrically in between parallel walls having either Neumann or Dirichlet conditions [3,11–13]. The obvious difference is indeed the boundary condition at infinity being replaced by a boundary condition at a finite distance, hence the similarity remains limited to the perfectly evanescent RB waves whose dispersion lies below the sound cone. The two-dimensional problem of acoustic scattering of an incident plane wave by a semi-infinite array of either rigid or soft circular scatterers [1,2,14–16] reveals the existence of complex eigenfrequencies, corresponding to leaky, radiating wave solutions, whose dispersion extends inside the sound cone [17]. It is the purpose of this Letter to show that leaky Rayleigh-Bloch waves can be guided inside the sound cone and that guided bound states in the continuum arise, as a result of the combination of symmetry and periodicity. The concept of guided quasinormal modes (QNMs) is proposed to obtain the complex dispersion relation of leaky Rayleigh-Bloch waves [18] and the case of slow inclusions placed inside a fast medium is shown to be of particular interest.

Velocity or impedance contrast? We consider in the following that the time-harmonic wave field satisfies a scalar Helmholtz equation, which includes the case of acoustic waves and of surface waves on water, for instance. It is hence representative of the simplest wave models and could be extended to vector elastic waves in the future. For concreteness of the discussion, we use acoustic notations in the following. The wave equation is written

$$-(\boldsymbol{\nabla} - \imath k\hat{\boldsymbol{x}})\cdot[\bar{\rho}^{-1}(\boldsymbol{\nabla} - \imath k\hat{\boldsymbol{x}})p] - \omega^2\bar{B}^{-1}p = \sigma, \qquad (1)$$

with $\bar{\rho} = \rho/\rho_0$ the mass density relative to the host medium; similarly, $\bar{B} = B/B_0$ is the relative elastic modulus. Both dimensionless quantities are functions of space coordinates (Fig. 1). σ is a body source term. The wave field has the dependence $p(x,y)\exp[\imath(\omega t - kx)]$, with $p(x,y)$ periodic along axis x and the primitive unit cell depicted in Fig. 1.

Rayleigh-Bloch waves are most often considered in the case of hard-wall boundaries inside a fluid medium. In this case a Neumann boundary condition along the edge of the inclusion applies (vanishing normal derivative of the wave field; $\partial_n p = 0$); alternatively, the Dirichlet boundary condition can also be considered (vanishing wave field; $p = 0$). Figure 2(a) displays the dispersion relation computed using the resolvent formalism [17]. The diagram shows the local density of states (LDOS) estimated from the response to a stochastic source σ in Eq. (1), for every point (k,ω) in dispersion space. In order to include scaling effects, the reduced wave number $\bar{k} = ka/(2\pi)$ and the reduced frequency $\bar{\omega} = \omega a/(2\pi v_0)$ are used, with $v_0 = \sqrt{B_0/\rho_0}$ the velocity in the host medium. As a note, in the different panels of Fig. 2 there is a slight asymmetry in LDOS values with respect to the X point; this spurious imbalance in the response results numerically from the limited resolution of the finite-element mesh used. Below the sound cone, i.e., within the nonradiative region of

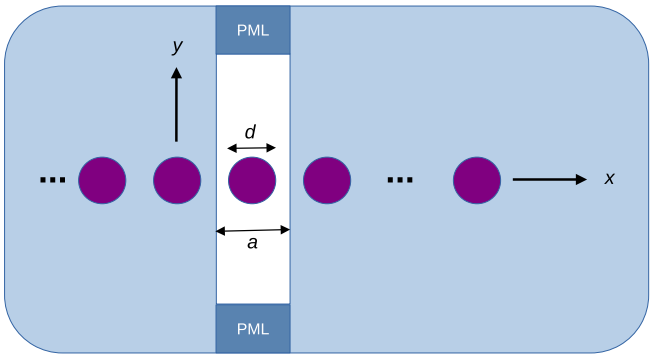

FIG. 1. Waveguide composed of a line of periodic inclusions in an open, infinite, host medium. The central portion shows the primitive unit cell with lattice constant a, terminated at the top and bottom by perfectly matched layers (PMLs). The diameter of cylindrical inclusions is $d = 0.6a$.

dispersion space, there is a single band giving the dispersion relation for Rayleigh-Bloch waves, for hollow inclusions with a hard-wall boundary. This is the usual solution considered in most papers on RB waves. The single band is folded at the X point of the Brillouin zone because of periodicity. A Bragg band gap opens for frequencies above it, but the upper band that closes this band gap is not apparent. We show in the following that it actually locates inside the sound cone and is strongly subject to radiation loss, so that it does not leave a visible trace in the resolvent band structure.

We now consider that the inclusions are filled with another fluid instead of being hollow. Heuristically, it can be understood that letting the dimensionless mass density of the inclusion tend to infinity results in a vanishing normal gradient of the wave field along the inclusion boundary [19]. Hence, we can consider a fictitious medium such that both $\bar{\rho}$ and $\bar{B}$ become very large in the same proportion. As a result the dimensionless acoustic velocity $\bar{v} = \sqrt{\bar{B}/\bar{\rho}} = 1$ remains constant whereas the dimensionless acoustic impedance $\bar{Z} = \sqrt{\bar{\rho}\bar{B}}$ increases in proportion. It can be checked that the dispersion relation for $\bar{\rho} = 100$ and $\bar{B} = 100$ in Fig. 2(b) is actually very close to the hollow inclusion case of Fig. 2(a). It is further instructive to test a case with $\bar{\rho} = \bar{B}$ not too large, in which case there is no velocity contrast but a moderate impedance contrast [$\bar{v} = 1$ and $\bar{Z} = 2$; see Fig. 2(c)]. There is still a single band, but the Bragg band gap tends to close toward the crossing point of right and left sound lines. It is generally observed that the dispersion of Rayleigh-Bloch waves follows closely the sound lines when $\bar{v} = 1$ and that the Bragg opening under the sound cone scales with the impedance contrast.

The situation changes if the inclusions are allowed to be slower than the host medium, in which case the dispersion of Rayleigh-Bloch waves shifts down in frequency as they localize more inside the inclusions [see Figs. 2(d)–2(f)]. Significantly, the second band above the Bragg band gap now appears clearly and extends inside the sound cone, i.e., inside the radiative region of dispersion space. The Bragg band gap itself exists even if the impedance contrast vanishes [case of Fig. 2(e)] and its opening is favored for $\bar{Z} < 1$ [Fig. 2(d)] as compared to the inverse setting $\bar{Z} > 1$ [Fig. 2(f)].

From the above observations, it can be concluded that the point in dispersion space around which the Bragg band gap opens for Rayleigh-Bloch waves can be moved down under the sound cone using slow inclusions ($\bar{v} < 1$). This results in

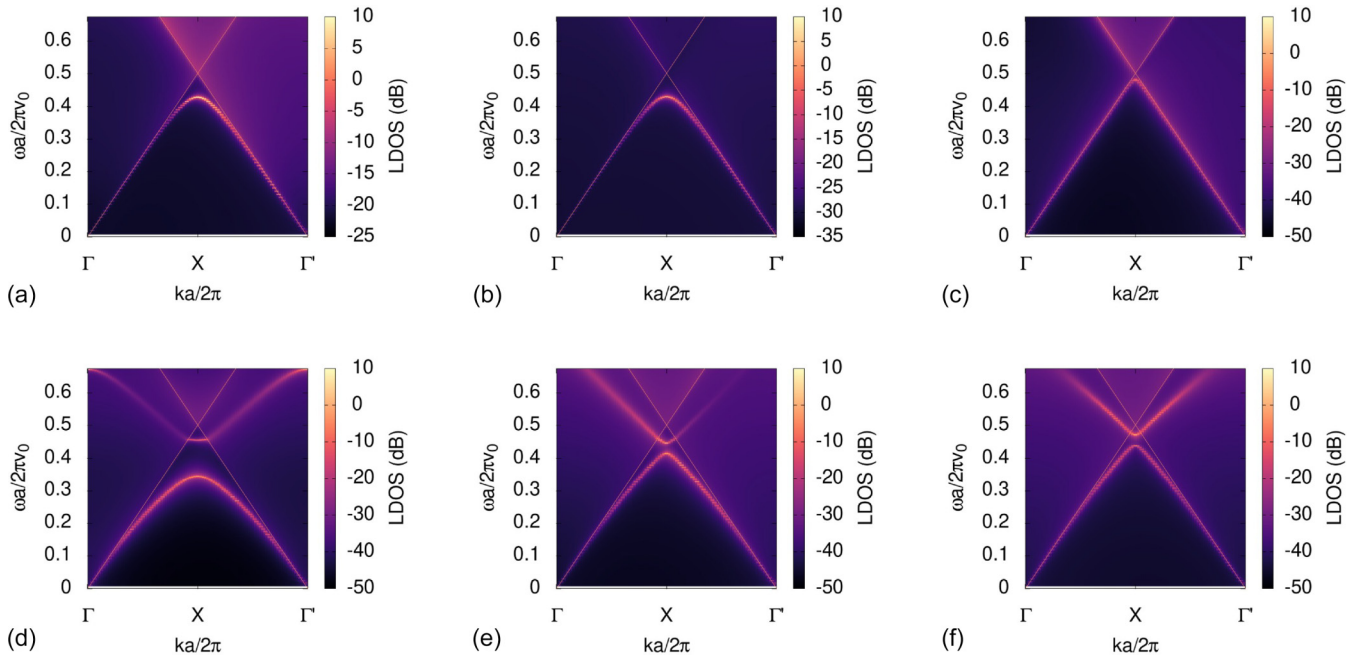

FIG. 2. Maps of the dispersion relation of Rayleigh-Bloch waves, computed using the resolvent band-structure method [17]. The color scale is for the local density of states (LDOS) estimated from the response to a stochastic source term. Panels are for (a) hollow inclusions satisfying a Neumann boundary condition along their edge, (b) inclusions with $\bar{\rho} = \bar{B} = 100$ ($\bar{v} = 1$ and $\bar{Z} = 100$), (c) inclusions with $\bar{\rho} = \bar{B} = 2$ ($\bar{v} = 1$ and $\bar{Z} = 2$), (d) inclusions with $\bar{\rho} = 1$ and $\bar{B} = 1/4$ ($\bar{v} = 1/2$ and $\bar{Z} = 1/2$), (e) inclusions with $\bar{\rho} = 2$ and $\bar{B} = 1/2$ ($\bar{v} = 1/2$ and $\bar{Z} = 1$), and (f) inclusions with $\bar{\rho} = 4$ and $\bar{B} = 1$ ($\bar{v} = 1/2$ and $\bar{Z} = 2$).

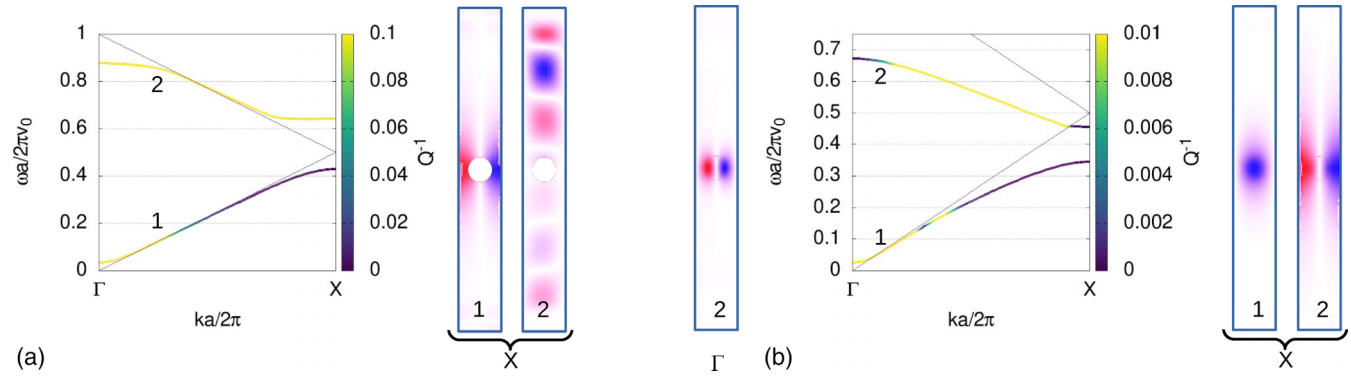

FIG. 3. Complex dispersion relation for leaky Rayleigh-Bloch waves treated as guided quasinormal modes. The color scale is for the inverse of the quality factor. (a) For hollow inclusions [same conditions as in Fig. 2(a)] the first band is guided but the second band, extending inside the sound cone, is always strongly leaky. (b) For filled inclusions with $\bar{\rho} = 1$ and $\bar{B} = 1/4$ [same conditions as in Fig. 2(d)] the dispersion of the second band is lossless at both the X and the Γ points. The latter solution is a bound state in the continuum (BIC) whereas the former is a guided wave. The real part of the pressure field of guided QNM solutions is shown within the primitive unit cell at high-symmetry points.

the second or folded band to be much less leaky than in the usual case of hollow inclusions. The opening of the Bragg band gap is then favored by decreasing the relative acoustic impedance of the inclusions ($\bar{Z} < 1$).

Complex dispersion relation. We now attempt to describe leaky RB waves that are partially guided along the chain of inclusions. The concept of quasinormal mode (QNM) [20,21] is used to quantify the effect of radiation loss of a phononic resonator in an open medium [22]. For a QNM with a complex frequency ω, in particular, the quality factor of the resonance is defined as $Q = \mathrm{Re}(\omega)/2\,\mathrm{Im}(\omega)$. Bloch waves are the eigenfunctions of a periodic, lossless medium and the band structure is composed of their dispersion relation. Here, we describe damped resonances in the resolvent band structure as quasinormal Bloch waves, their complex eigenfrequencies defining complex bands $\omega_n(k)$. The practical algorithm described in Ref. [22] to obtain a single QNM is here modified to track the complex dispersion relation of guided QNMs as a function of the wave number. Consider a discrete sequence $(k_i, i = 0 \cdots m)$ sampling the k axis. Starting from a given point (k_i, ω_i) of dispersion space, the iteration converges fast toward the closest QNM at fixed k_i, yielding an estimate of the complex frequency $\omega_n(k_i)$ as well as of the field $p_n(x; k_i)$ of the QNM of interest. If $i = 0$, the starting frequency has to be guessed from the resolvent band structure and a stochastic source is chosen for initialization. For step $i > 0$, the starting frequency and the QNM candidate can be chosen as $\omega_n(k_{i-1})$ and $p_n(x; k_{i-1})$, and the iteration will converge to $\omega_n(k_i)$ and $p_n(x; k_i)$. Repeating this elementary step, the complex band is easily and efficiently obtained, since each iteration requires the solution of only a few linear systems.

Considering the case of Rayleigh-Bloch waves for hollow inclusions in Fig. 2(a), the complex band tracking algorithm readily produces the complex dispersion relation displayed in Fig. 3(a). The first band, that was visible in the resolvent band structure, is lossless (purely real) since it belongs to guided modes under the sound cone. It is seen that the QNM tracking algorithm does not function very well at low frequencies and low wave numbers, since the solution extends laterally very widely inside the PML. In this case, the QNM cannot be clearly separated from PML eigenmodes and can be lost by the tracking algorithm. Note that this limitation does not affect

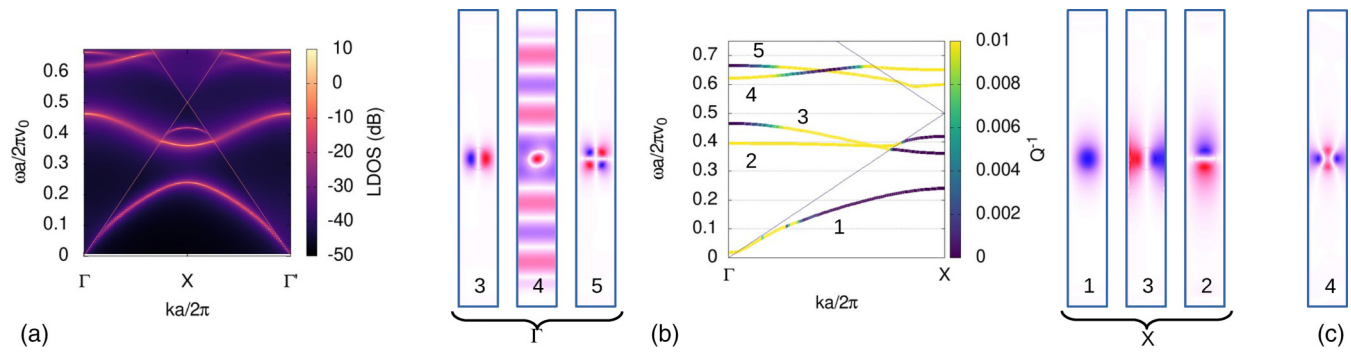

FIG. 4. Dispersion relation of Rayleigh-Bloch waves for inclusions with $\bar{\rho} = 1$ and $\bar{B} = 1/9$ ($\bar{v} = 1/3$ and $\bar{Z} = 1/3$). (a) Map of the dispersion relation computed using the resolvent band structure method [17]. The color scale is for the local density of states (LDOS) estimated from the response to a stochastic source term. (b) Complex dispersion relation for leaky Rayleigh-Bloch waves treated as guided quasinormal modes. The color scale is for the inverse of the quality factor. The real part of the pressure field of guided QNM solutions is shown within the primitive unit cell at high-symmetry points. Examples of bound states in the continuum (BIC) are shown for bands 3 and 5 at the Γ point. (c) The Rayleigh-Bloch wave of band 4 at $ka/(2\pi) \approx 0.236$ inside the first Brillouin zone is also a BIC.

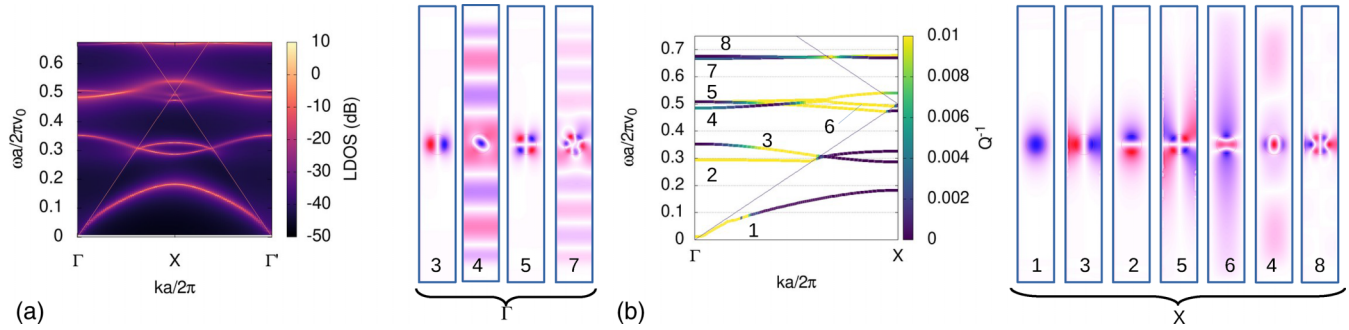

FIG. 5. Dispersion relation of Rayleigh-Bloch waves for inclusions with $\bar{\rho} = 1$ and $\bar{B} = 1/16$ ($\bar{v} = 1/4$ and $\bar{Z} = 1/4$). (a) Map of the dispersion relation computed using the resolvent band structure method [17]. The color scale is for the local density of states (LDOS) estimated from the response to a stochastic source term. (b) Complex dispersion relation for leaky Rayleigh-Bloch waves treated as guided quasinormal modes. The color scale is for the inverse of the quality factor. The real part of the pressure field of guided QNM solutions is shown within the primitive unit cell at high-symmetry points. Examples of bound states in the continuum (BIC) are shown for bands 3 and 5 at the Γ point, and band 8 at the X point.

the computation of the resolvent band structure, anyway. The second complex band has a low-quality factor for all wave numbers and could not be seen in the resolvent band structure, since its response is very low. Moving the excitation frequency to the complex plane however makes it apparent.

Considering the slow inclusion case of Fig. 2(d), the same procedure leads to the complex dispersion relation displayed in Fig. 3(b). The first complex band is similar to the one in Fig. 3(a), though the wave field localizes on the inclusions rather than in between them. Significantly, since the second complex band has moved down in frequency, it first appears as lossless after the folding at the X point of the Brillouin zone $[ka/(2\pi) = 0.5]$ but becomes lossy as it enters the sound cone. Surprisingly, loss tends to 0 ($Q \longrightarrow \infty$) at the Γ point $[ka/(2\pi) = 0]$ for this second band. At this point, the QN Bloch wave becomes a bound state in the continuum (BIC) [23–25], since it it lossless although its dispersion lies inside the sound cone. The BIC property here results from a combination of symmetry and periodicity, as the QN Bloch wave is a collective vibration state of the periodic, infinite chain of inclusions. This is in contrast to band folding considered as the BIC generation mechanism [26].

We next increase the material contrast in Fig. 4. The frequency decrease of the dispersion of QN Bloch waves is stronger and a total of five bands is observed in the frequency range of interest, the first three of them being guided Rayleigh-Bloch waves, i.e., extending below the sound cone. Each new band is clearly associated with a particular resonance of the inclusion and has a definite symmetry, in particular dictated by the azimuthal number m of isolated QNMs discussed in the Appendix. Band 3 ($m = 1$) and band 5 ($m = 2$) both hold a BIC at the Γ point. Surprisingly, another BIC occurs for band 4 for a k value in between the high-symmetry points Γ and X, at $ka/(2\pi) \approx 0.236$. As Fig. 4(c) shows, $m = 2$ for this BIC also.

Increasing again the material contrast in Fig. 5, the overall trends are confirmed. There are now eight complex bands, with the additional appearance of an $m = 3$ resonance leading to a BIC at both the Γ and the X point (band 8). Band 4 again holds a BIC for a k value in between the high-symmetry points Γ and X, at $ka/(2\pi) \approx 0.172$, again with $m = 2$. The corresponding modal shape, not shown in Fig. 5, is very similar to the one in Fig. 4(c).

Conclusion. The complex dispersion relation of Rayleigh-Bloch waves has been discussed for both the traditional case of hollow inclusions and the case of slow inclusions in a homogeneous propagation medium. The introduction of slow inclusions, in particular, results in the appearance of localized resonances whose frequencies down-shift when velocity decreases, leading to the formation of additional Rayleigh-Bloch wave bands. The key to the description of leaky Bloch waves that are partially guided along a periodic chain of inclusions is here the concept of phononic quasinormal modes, that has been extended to include the case of guided waves. For a fixed real wave number, QNMs have a complex eigenfrequency that can be estimated by a search inside the complex dispersion plane. As a result, both the eigenmodes and the quality factor Q of the associated resonance are obtained. Interestingly, for certain values of the wave number and as a result of its symmetry, a guided QNM can uncouple from bulk radiation modes, allowing to identify it as a bound state in the continuum (BIC).

The material system considered in the present derivation—a fluid in a fluid—may seem difficult to realize experimentally. The reason for this choice was to handle the Helmholtz equation for scalar waves, one of the simplest among the class of wave equations. The results discussed here, however, already apply to the case of pure-shear out-of-plane elastic waves in solids, for instance, or of transverse-electric and transverse-magnetic electromagnetic waves. It remains to extend the exposed method to vector Rayleigh-Bloch waves in solids and in three dimensions, but the concept incidentally shines light on previous experimental [27] and numerical [28] results for surface acoustic waves (SAWs) guided along a chain of pillars on a substrate.

Acknowledgments. This work was supported by the Agence Nationale de la Recherche, EIPHI Graduate School (Grant No. ANR-17-EURE-0002). Finite-element computations were performed with FREEFEM++ [29].

Data availability. The data that support the findings of this article are openly available [30].

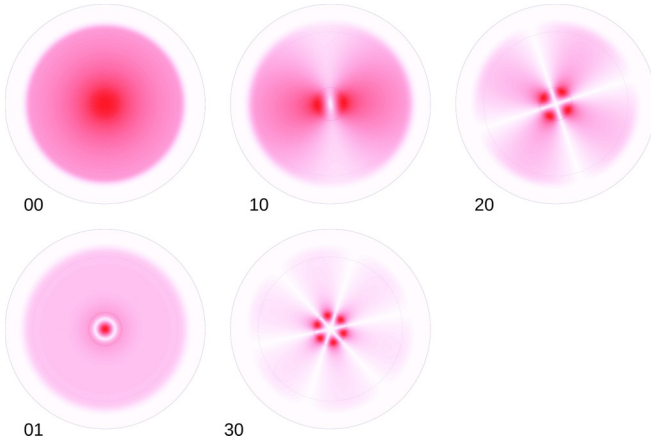

FIG. 6. Quasinormal modes of isolated slow inclusions with diameter $d = 0.6a$. The labels refer to m and n, the azimuthal and radial numbers. Quasinormal modes are computed for the case $\bar{\rho} = 1, \bar{B} = 1/16$ of Table I and their modulus is displayed after normalization.

Appendix: QNM symmetry. The numerical observations made in the above section on the complex dispersion relation hint at the importance of quasinormal mode symmetry. Rayleigh-Bloch waves, as a particular type of Bloch waves, are collective, periodic excitations. As such they convey the symmetry of both the primitive unit cell and of the periodic lattice. In this Appendix we examine the symmetry of the former, given here by the symmetry of the inclusion.

Consider a single inclusion embedded in an infinite surrounding acoustic medium. It supports quasinormal modes describing vibrations localized around the inclusion but radiating energy away from it. This situation can be represented numerically using a PML surrounding completely the inclusion [22]. The first five QNMs that are found numerically in the frequency range of interest are displayed in Fig. 6. Considering the central symmetry of the problem, the acoustic wave equation separates in polar coordinates (r, θ). As a result, QNMs are indexed by an azimuthal number m and a radial number n, so that $p_{mn}(r, \theta) = \exp(\imath m\theta)P_n(r)$. They are doubly degenerate if $m > 0$. The numerical QNM solutions thus converge to a superposition with azimuthal indices $\pm m$ in this case. The result of the classification of QNMs is summarized in Table I. Quality factors are either low or moderate, because of radiation toward infinity, and improve with the azimuthal number. The reduced QNM frequencies are in a clear correspondence with the Rayleigh-Bloch bands of Figs. 3(b), 4, and 5. The BICs discussed in the above section on the complex dispersion relation are found for azimuthal numbers $m > 0$.

TABLE I. Properties of quasinormal modes of isolated slow inclusions with diameter $d = 0.6a$. m and n are the azimuthal and radial numbers, respectively.

Contrast	mn	00	10	20	01	30
$\bar{\rho} = 1, \bar{B} = 1/4$	$\bar{\omega}$	0.39	0.59	0.96		1.26
	Q	1.5	3.4	4.7		10.5
$\bar{\rho} = 1, \bar{B} = 1/9$	$\bar{\omega}$	0.13	0.41	0.65	0.69	0.88
	Q	1.6	3.4	16.1	5.1	50.3
$\bar{\rho} = 1, \bar{B} = 1/16$	$\bar{\omega}$	0.11	0.30	0.49	0.53	0.67
	Q	2.0	6.7	30.1	8.5	171.7

[1] L. G. Bennetts and M. A. Peter, Rayleigh–Bloch waves above the cutoff, J. Fluid Mech. **940**, A35 (2022).
[2] M. A. Peter, M. H. Meylan, and C. M. Linton, Water-wave scattering by a periodic array of arbitrary bodies, J. Fluid Mech. **548**, 237 (2006).
[3] C. M. Linton and P. McIver, Embedded trapped modes in water waves and acoustics, Wave Motion **45**, 16 (2007).
[4] R. Porter and D. V. Evans, Rayleigh–Bloch surface waves along periodic gratings and their connection with trapped modes in waveguides, J. Fluid Mech. **386**, 233 (1999).
[5] L. G. Bennetts, M. A. Peter, and F. Montiel, Localisation of Rayleigh–Bloch waves and damping of resonant loads on arrays of vertical cylinders, J. Fluid Mech. **813**, 508 (2017).
[6] C. M. Linton and M. McIver, The existence of Rayleigh–Bloch surface waves, J. Fluid Mech. **470**, 85 (2002).
[7] G. J. Chaplain, M. P. Makwana, and R. V. Craster, Rayleigh–Bloch, topological edge and interface waves for structured elastic plates, Wave Motion **86**, 162 (2019).
[8] B. Maling and R. V. Craster, Whispering Bloch modes, Proc. R. Soc. A **472**, 20160103 (2016).
[9] G. P. Ward, J. D. Smith, A. P. Hibbins, J. R. Sambles, and T. A. Starkey, Gapless dispersion of acoustic line modes with glide symmetry, Phys. Rev. B **105**, 245401 (2022).
[10] G. J. Chaplain, S. C. Hawkins, M. A. Peter, L. G. Bennetts, and T. A. Starkey, Acoustic lattice resonances and generalised Rayleigh–Bloch waves, Commun. Phys. **8**, 37 (2025).
[11] D. V. Evans and R. Porter, Trapped modes embedded in the continuous spectrum, Q. J. Mech. Appl. Math. **51**, 263 (1998).
[12] D. V. Evans and R. Porter, Trapping and near-trapping by arrays of cylinders in waves, J. Eng. Math. **35**, 149 (1999).
[13] H. D. Maniar and J. N. Newman, Wave diffraction by a long array of cylinders, J. Fluid Mech. **339**, 309 (1997).
[14] C. M. Linton and I. Thompson, Resonant effects in scattering by periodic arrays, Wave Motion **44**, 165 (2007).
[15] M. A. Peter and M. H. Meylan, Water-wave scattering by a semi-infinite periodic array of arbitrary bodies, J. Fluid Mech. **575**, 473 (2007).
[16] I. Thompson, C. M. Linton, and R. Porter, A new approximation method for scattering by long finite arrays, Q. J. Mech. Appl. Math. **61**, 333 (2008).
[17] V. Laude and M. E. Korotyaeva, Stochastic excitation method for calculating the resolvent band structure of periodic media and waveguides, Phys. Rev. B **97**, 224110 (2018).
[18] K. Matsushima, L. G. Bennetts, and M. A. Peter, Tracking Rayleigh–Bloch waves swapping between Riemann sheets, Proc. R. Soc. A **480**, 20240211 (2024).
[19] A mathematical derivation can be obtained by applying the divergence theorem to a closed contour encircling locally the inclusion boundary.

[20] E. S. C. Ching, P. T. Leung, A. M. Van Den Brink, W. M. Suen, S. S. Tong, and K. Young, Quasinormal-mode expansion for waves in open systems, Rev. Mod. Phys. **70**, 1545 (1998).

[21] T. Wu, M. Gurioli, and P. Lalanne, Nanoscale light confinement: The Q's and V's, ACS Photonics **8**, 1522 (2021).

[22] V. Laude and Y.-F. Wang, Quasinormal mode representation of radiating resonators in open phononic systems, Phys. Rev. B **107**, 144301 (2023).

[23] F. H. Stillinger and D. R. Herrick, Bound states in the continuum, Phys. Rev. A **11**, 446 (1975).

[24] C. W. Hsu, B. Zhen, A. D. Stone, J. D. Joannopoulos, and M. Soljačić, Bound states in the continuum, Nat. Rev. Mater. **1**, 16048 (2016).

[25] S. An, T. Liu, L. Cao, Z. Gu, H. Fan, Y. Zeng, L. Cheng, J. Zhu, and B. Assouar, Multibranch elastic bound states in the continuum, Phys. Rev. Lett. **132**, 187202 (2024).

[26] W. Wang, Y. K. Srivastava, T. C. Tan, Z. Wang, and R. Singh, Brillouin zone folding driven bound states in the continuum, Nat. Commun. **14**, 2811 (2023).

[27] L. Socié, S. Benchabane, L. Robert, A. Khelif, and V. Laude, Surface acoustic wave guiding in a diffractionless high aspect ratio transducer, Appl. Phys. Lett. **102**, 113508 (2013).

[28] M. Al Lethawe, M. Addouche, S. Benchabane, V. Laude, and A. Khelif, Guidance of surface elastic waves along a linear chain of pillars, AIP Adv. **6**, 121708 (2016).

[29] F. Hecht, New development in FREEFEM++, J. Numer. Math. **20**, 251 (2012).

[30] V. Laude, "Complex dispersion relation of Rayleigh-Bloch waves trapped by slow inclusions (2025)" [DataSet], Zenodo, doi:10.5281/zenodo.15363736..